

## Na<sub>2</sub>Ti<sub>3</sub>O<sub>7</sub> nano fibres as an anode material for rechargeable Na-ion batteries

R. I. C. Niroshan Karunarathne<sup>1,2</sup>, Thusan Pathirana<sup>1,2</sup>, H. W. M. A. C. Wijayasinghe<sup>1,2\*</sup> and M. A. K. L. Dissanayake<sup>1,2</sup>

<sup>1</sup> National Institute of Fundamental Studies, Kandy, Sri Lanka

<sup>2</sup> Postgraduate Institute of Science, University of Peradeniya, Peradeniya, Sri Lanka

Received: 4/8/2017; Accepted: 03/04/2018

**Abstract:** Na<sub>2</sub>Ti<sub>3</sub>O<sub>7</sub> has been known for a long time and studied for several applications in sensors, catalysis and in toxic waste removal. The applicability of Na<sub>2</sub>Ti<sub>3</sub>O<sub>7</sub> as an anode material for rechargeable Na-ion batteries was investigated in this study. Na<sub>2</sub>Ti<sub>3</sub>O<sub>7</sub> nano fibers were synthesized by hydrothermal technique and characterized by using X-ray diffraction and scanning electron microscopy. The results show that spherical Na<sub>2</sub>Ti<sub>3</sub>O<sub>7</sub> materials consisting of tiny nano fibers have been formed. The electrochemical characterization was performed with Na metal electrode in coin half-cells fabricated in an Ar inert atmosphere. The galvanostatic charge-discharge measurements in the voltage range of 0.02 - 1.9 V revealed the initial discharge capacity of 787.2 mAhg<sup>-1</sup> at C / 10 rate and the discharge capacity was decreased to 55 mAhg<sup>-1</sup> over 30 cycles. The results suggest that the crystalline Na<sub>2</sub>Ti<sub>3</sub>O<sub>7</sub> nano fibers are suitable to be used as an anode material in rechargeable Na-ion batteries.

**Keywords:** Na-ion battery, anode material, hydro thermal technique, Na<sub>2</sub>Ti<sub>3</sub>O<sub>7</sub> nano fiber.

### INTRODUCTION

Li-ion batteries are the most dominant power sources used in portable electronic devices and in electric vehicles due to their high energy density and long cycle life. In addition, they are also being developed for applications in the smart grid to store excess electrical energy for future consumption. However, the cost of Li-ion batteries continues to increase with increasing applications, largely due to the limited lithium resources available in the earth's crust. In particular, for large scale applications of Li-ion batteries, the cost of the raw materials is one of the most important factors to be considered. Due to these factors, in recent years, extensive attention has been paid for the development of sodium-ion batteries as an alternative for the expensive Li-ion batteries, mainly due to high abundance of Na and its similarity to Li in many chemical and physical properties. Indeed, if electrochemical performance of Li-ion batteries could be replaced by Na-ion batteries, the cost of rechargeable batteries could be dramatically reduced and large scale applications would also be more feasible (Wang *et al.*, 2013; Seung-Min *et al.*, 2013).

materials suitable for Na-ion batteries such as Na<sub>x</sub>CoO<sub>2</sub>, NaNi<sub>0.5</sub>Mn<sub>0.5</sub>O<sub>2</sub>, P2-Na<sub>2/3</sub>Ni<sub>1/3</sub>Mn<sub>2/3</sub>O<sub>2</sub>, P2-Na<sub>0.875</sub>Li<sub>0.17</sub>Ni<sub>0.21</sub>Mn<sub>0.64</sub>O<sub>2</sub> and phosphates (*i.e.* NaMPO<sub>4</sub> where M = Fe, Mn, etc.) have been reported (Huilin *et al.*, 2013; Luyuan *et al.*, 2015). However, only few anode materials such as carbon black, mesocarbon microbeads and hard carbon have been investigated and reported for Na-ion batteries (Wang *et al.*, 2013; Yunhua *et al.* 2013). In addition, some alloys such as nano composites of Sb/C, Sn/C and SbSn/C have been reported for their high energy capacities (Huilin *et al.*, 2013; Seung-Min *et al.*, 2013; Yunhua *et al.*, 2013). However, they have raised some safety issues due to their high volume expansion during the charging-discharging process. Hence, the development of new compatible anode materials to be used for Na-ion batteries has become an important research area at present.

Recently, some titanium metal based compounds such as amorphous TiO<sub>2</sub> nano tubes (Xiong *et al.*, 2011; Huilin *et al.*, 2013) spinal Li<sub>4</sub>Ti<sub>5</sub>O<sub>12</sub> and Na<sub>2</sub>Ti<sub>3</sub>O<sub>7</sub> (Wang *et al.*, 2013; Wu *et al.*, 2015) have been investigated for Na-ion battery applications. Out of these Na<sub>2</sub>Ti<sub>3</sub>O<sub>7</sub> has received a greater attention as an anode material for Na-ion batteries due to its high ionic exchange ability and high Na<sup>+</sup> ion conductivity (Huilin *et al.*, 2013). In this material, the sodium ions in the interlayer space in the zigzag layered structure of titanium oxygen octahedra (Senguttuvan *et al.* 2011) can easily be exchanged with the possibility of good electrochemical performance. These titanium-based materials have been synthesized via a solid state reaction method, micro-emulsion method and hydrothermal reaction method (Zhang *et al.*, 2008).

The hydrothermal method is a convenient and well established technique for synthesizing nano-scale crystalline materials at low temperature under high pressure (Chen *et al.*, 2007). Nanostructured materials have shown improved power and energy densities compared with their bulk counterparts due to enhanced kinetics and large effective surface area (Xiong *et al.*, 2011). Hence, extensive research has been focused on synthesizing nano materials for the electrode in energy storage devices (By Kyu *et al.*, 2005).

In a recent study by Zhang *et al.* (2014), Na<sub>2</sub>Ti<sub>3</sub>O<sub>7</sub> nanotubes interwoven 3-D spider web-like growth on Ti

Some layered transition metal oxide based cathode

\*Corresponding Author's Email: [athula@ifs.ac.lk](mailto:athula@ifs.ac.lk)

 <http://orcid.org/0000-0003-0227-6580>



flakes were directly synthesized by hydrothermal conditions and successfully tested as an anode material for Na-ion batteries without adding any binders. In and another study on evaluation of the Solid-electrolyte interphase (SEI) in  $\text{Na}_2\text{Ti}_3\text{O}_7$  synthesized through an ordinary ceramic route was reported (Miguel *et al.*, 2015). Both these studies suggested the poor capacity retention in the initial cycles is due to the formation of SEI on both inner and outer surface of the  $\text{Na}_2\text{Ti}_3\text{O}_7$  nanotubes (Zhang *et al.*, 2014; Miguel *et al.*, 2015). However, the performance of  $\text{Na}_2\text{Ti}_3\text{O}_7$  prepared, in the form of nano fibers, by hydrothermal technique has not yet been reported elsewhere to the knowledge of the authors. Therefore in this present study,  $\text{Na}_2\text{Ti}_3\text{O}_7$  nano fibers were successfully synthesized through a low temperature hydrothermal technique by using low cost raw materials such as  $\text{TiO}_2$  and  $\text{NaOH}$  and its electrochemical performance was investigated.

## METHODOLOGY

### Preparation of Materials

$\text{Na}_2\text{Ti}_3\text{O}_7$  nano fibers were synthesized at low temperature (150 °C) by the hydrothermal synthesis technique. Initially, 2 g of anatase  $\text{TiO}_2$  (99%, Sigma-Aldrich) was dispersed in 10 ml of aqueous  $\text{NaOH}$  solution (10 mol  $\text{dm}^{-3}$ ) in a teflon chamber. After being continuously stirred for 2 hours, the teflon chamber was sealed and kept in a stainless steel autoclave and heated at 150 °C for 24 hours. The precipitate was collected and subsequently stirred in distilled water to form nano fibers dispersed in water. The mixture was centrifuged and then dried in an oven at 120 °C for 24 hours.

### Material Characterization

The structure and morphology of the prepared  $\text{Na}_2\text{Ti}_3\text{O}_7$  fine powders were characterized by X-ray diffraction (XRD, Rigaku Ultima IV X-ray Diffractometer equipped

with a Cu anode and dual detectors) and scanning electron microscopy (SEM, ZEISS Scan Electron Microscope attached with Energy-dispersive X-ray spectroscopy)

### Cell Preparation for Electrochemical Characterization

The electrochemical performance was carried out using coin cells assembled in an inert Ar atmosphere. The working electrode was fabricated by using the active material of  $\text{Na}_2\text{Ti}_3\text{O}_7$  nano fibers with Super P-carbon (Erachem Europe) and PVDF (polyvinylidene fluoride, Kynar HSV 900) binder in the weight ratio of 70:15:15 and thoroughly mixing in N-methyl-2-pyrrolidone (Sigma Aldrich, anhydrous 99.5%) by using 0.2 mm stainless steel balls in a ball mill (50 rpm, 1 hour) to create a uniform slurry. The slurry was then coated uniformly on a copper foil by using a stainless steel coating bar and subsequently dried at 120 °C for over 12 hours. Circular shaped electrodes of 15 mm diameter were punched from the resulting coatings. The cells were assembled inside the argon filled glove box ( $[\text{O}_2] < 1$  ppm,  $[\text{H}_2\text{O}] < 1$  ppm), considering the active material electrode was the working electrode while Na metal was the both counter and reference electrode. The electrolyte used was 1 M  $\text{NaPF}_6$  (98%, Sigma-Aldrich) in ethylene carbonate (EC) (Daejung)/ diethylene carbonate (DEC) (Daejung)/ fluoroethylene carbonate (FEC) (Novolyte Technologies) in the volume ratio of 3:6:1. A blown microfiber (BMF) from Whatman was used as separator. The assembled coin cells were tested with a Landt automated battery tester under different current densities between cutoff voltages of 0.02 and 1.9 V versus Na.

## RESULTS AND DISCUSSION

### Structural Identification of the Prepared Sample

The SEM images of the as-prepared  $\text{Na}_2\text{Ti}_3\text{O}_7$  material synthesized by hydrothermal synthesis technique are

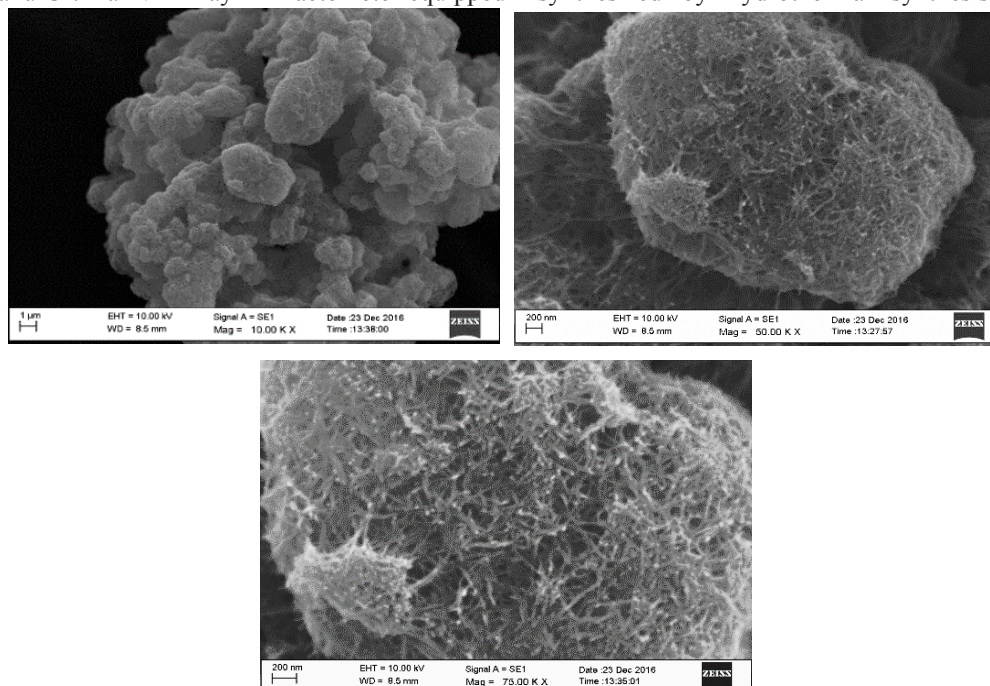


**Figure 1.** The SEM images of the  $\text{Na}_2\text{Ti}_3\text{O}_7$  nanofibers synthesized by hydrothermal synthesis technique.

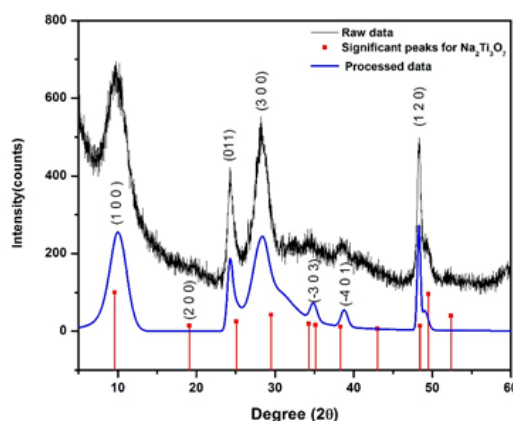


**Figure 2.** The XRD patterns of  $\text{Na}_2\text{Ti}_3\text{O}_7$  fibers synthesized by hydrothermal method.

presented in Figure 1. The SEM images indicate the existence of spherical shapes particles which contains thousands of nano fibers gathered and interweaved together to form porous microspheres with average diameter of 2  $\mu\text{m}$ . A fiber shaped morphology with around 10-30 nm in diameter and around 200-500 nm in length can be observed. This porous microsphere structure could increase the specific surface area and electrolyte-material interface that might be supportive to enhance its electrochemical performance. In addition, the stability of the structure could be maintained during discharge-charge cycling process without any volume expansion.

The XRD pattern (Cu  $K\alpha$ ) of the as-prepared  $\text{Na}_2\text{Ti}_3\text{O}_7$  nano fiber is shown in Figure 2 and corresponding peaks are compared with the standard peak patterns of  $\text{Na}_2\text{Ti}_3\text{O}_7$  crystalline material (PDF No. 00-059-0666). The main peaks of the prepared material are well matched with the standard XRD pattern of  $\text{Na}_2\text{Ti}_3\text{O}_7$  phase. Peak broadening might be due to the fine particle size of the material. The existence of the well-crystallized phase can be seen without any traces of impurity phases. The crystalline structure of  $\text{Na}_2\text{Ti}_3\text{O}_7$  is formed with zigzag layers of titanium-oxygen octahedra and with two sodium ions located in the interlayer space (Wang *et al.*, 2013). Within the interlayer space more  $\text{Na}^+$  ions can be occupied during the  $\text{Na}^+$  ions intercalation process without interrupting its structural stability (Kolen'ko *et al.*, 2006).

### Electrochemical Characterization

Upon the initial discharge process, two voltage peaks at 1.105 and 0.488 V appeared in CV measurements as shown in the Figure 3 (c) which might be associated with side reactions of the electrolyte reduction and formation of Solid Electrolyte Interface (SEI) layer. However, the peaks disappeared in the subsequent charge-discharge process as can be seen in the Figure. The Electrochemical performance of  $\text{Na}_2\text{Ti}_3\text{O}_7$  fibers performed at C / 10 rate in the voltage range of 0.02-1.9 vs  $\text{Na}^+/\text{Na}$  is shown in the Figure 3 (a). It is clearly see that  $\text{Na}_2\text{Ti}_3\text{O}_7$  fibers delivered 787  $\text{mAhg}^{-1}$  of

initial discharge capacity which is more than twice of the expected theoretical capacity of 311  $\text{mAhg}^{-1}$ . This high initial discharge capacity may be due to the formation of the Solid Electrolyte Interface (SEI) layer in-between electrode and electrolyte. As it is clearly seen that the second discharge capacity value dropped down to 120  $\text{mAhg}^{-1}$ , suggesting that during initial discharge process, a considerable amount of intercalated Na ions have contributed to the formation of SEI interface and it was difficult to extract them upon following charging cycles (Miguel *et al.*, 2015). The cyclic performance is shown in Figure 3 (c). It can be observed that the charge-discharge capacity was maintained at around 50  $\text{mAhg}^{-1}$  during the first 30 cycles. However, it is interesting to note that the Columbic efficiency was achieved more than 95% after the first few cycles.

### CONCLUSION

The  $\text{Na}_2\text{Ti}_3\text{O}_7$  nanofibers were synthesized by low temperature hydrothermal technique at 150  $^{\circ}\text{C}$  and its electrochemical characterization was studied in order to determine its applicability as an anode material for Na-ion batteries. The XRD study revealed the existence of the crystalline phase formed without any residual phases. These porous aggregated globular particles contain a large number of tiny nano fibers interweaved which increases the effective specific surface area of the  $\text{Na}_2\text{Ti}_3\text{O}_7$  nano fiber particles. The electrochemical studies revealed that  $\text{Na}^+$  ions can be reversibly intercalated into  $\text{Na}_2\text{Ti}_3\text{O}_7$  nanofibers with high initial discharge capacity. However, discharge capacity dropped abruptly after initial discharge state which could be due to the formation of SEI layer. However, the discharge capacity was maintained at 55  $\text{mAhg}^{-1}$  over the first 30 cycles. This study has revealed the ability to use  $\text{Na}_2\text{Ti}_3\text{O}_7$  nanofibers as an anode material for Na-ion rechargeable batteries. However, further improvements are needed to enhance the gravimetric capacity of these materials without interrupting its structural stability.

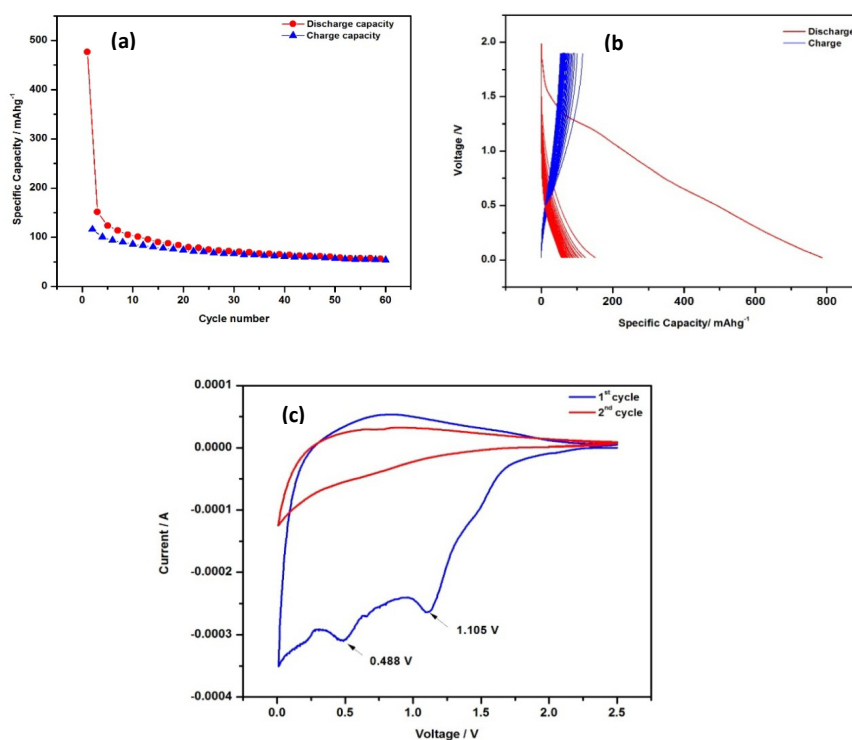


**Figure 3:** Electrochemical performance of Na<sub>2</sub>Ti<sub>3</sub>O<sub>7</sub> nanofibers. (a) The charge-discharge capacity versus cycle number at a current rate of C/10. (b) Initial galvanostatic charge-discharge curves at a current rate of C/10 in the voltage range of 0.02-1.9 V versus Na<sup>+</sup>/Na. (c) Cyclic Voltammograms of Na<sub>2</sub>Ti<sub>3</sub>O<sub>7</sub> at 0.05 mVs<sup>-1</sup> in the voltage range 0.0-2.5 V.

## REFERENCES

- By Kyu, T.L., Lytle, C.J., Ergang, N.S., Oh, S.M. and Stein, A. (2005). Synthesis and rate performance of monolithic macroporous carbon electrodes for lithium-ion batteries. *Advanced functional Materials* **15**: 547-556.
- Cheng, J., Wang, S. and Whittingham, M.S. (2007). Hydrothermal synthesis of cathode materials. *Journal of Power Source* **174**: 442-448.
- Huilin, P., Lu, X., Hu, Y., Li, H., Yang, X. and Chen, J.L. (2013). Sodium storage and transport properties in layered Na<sub>2</sub>Ti<sub>3</sub>O<sub>7</sub> for room-temperature Sodium-ion batteries. *Advanced Energy Materials* **3**: 1186-1194.
- Kolen'ko, Y., Kovnir, K.A., Gavrilov, A.I., Garshev, A.V., Frantti, J., Lebedev, O.I., Churagulov, B.R., Tndeloo, G.V. and Yoshimura M. (2006). Hydrothermal synthesis and characterization of nanorods of various titanates and Titanium dioxide. *Journal of Physical Chemistry* **110**: 4030-4038.
- Luyuan, P.W., Yu, L., Wang, X., Srinivasan, M. and Xu, Z.J. (2015). Recent developments of electrode materials for sodium ion batteries. *Journal of Material Chemistry* **3**: 9353-9378.
- Munoz-Marquez, M.A., Zarrabeitia, M., Castillo-Martinez E., Eguia-Barrio, A., Rojo, T., and Casas-Cabanas M. (2015). Composition and Evolution of the Solid-Electrolyte Interphase in Na<sub>2</sub>Ti<sub>3</sub>O<sub>7</sub> Electrode for Na-ion Batteries: XPS and Auger Parameter Analysis. *ACS Appl. Mater. Interface* **14**: 7801-7808.
- Senguttuvan, P., Rouse, G., Seznec, V., Tarascon, J. and Palacin, M.R. (2011). Na<sub>2</sub>Ti<sub>3</sub>O<sub>7</sub>: Lowest voltage ever reported oxide insertion electrode for Sodium ion Batteries. *Chemistry of Materials* **23**: 4109-4111.
- Seung-Min, O., Myung, A., Jang, M., Scrosati, B., Hassoun, J. and Sun, Y. (2013). An advanced Sodium-ion rechargeable battery based on a tin-carbon layered oxide framework cathode. *Physical Chemistry Chemical Physics* **15**: 3827-3833.
- Wang, W., Yu, C., Lin, Z., Hou, J., Zhu, H. and Jiao, S. (2013). Microspheric Na<sub>2</sub>Ti<sub>3</sub>O<sub>7</sub> consisting of tiny nanotubes: an anode material for sodium-ion batteries with ultrafast charge-discharge rate. *Nanoscale* **5**: 594-599.
- Wu, D., Li, X., Xu, B., Twu, N., Liu, L. and Ceder, G. (2015). NaTiO<sub>2</sub>: A layered anode material for sodium-ion batteries. *Energy Environ. Sci.* **8**: 195-202.
- Xiong, X., Slater, M.D., Balasubramanian, M., Johnson, C.S. and Rajh, T. (2011). Amorphous TiO<sub>2</sub> nanotube anode for rechargeable Sodium ion batteries. *Journal of Physical Chemistry Letters* **2**: 2560-2565.
- Yunhua, X., Zhu, Y., Liu, Y. and Wang, C. (2013). Electrochemical performance of porous Carbon/Tin composite anode for Sodium-ion and Lithium-ion batteries. *Advanced Energy Materials* **3**: 128-133.
- Zhang, Y.J., Yan, W., Wu, Y.P. and Wang, Z.H. (2008). Synthesis of TiO<sub>2</sub> nanotubes coupled with CdS nanoparticles and production of hydrogen by photocatalytic water decomposition. *Materials Letters* **62**: 3846-3848.
- Zhang, Y., Guo, L., and Yang, S. (2014). Three-dimensional spider-web architecture assembled from Na<sub>2</sub>Ti<sub>3</sub>O<sub>7</sub> nanotubes as a high performance anode for a sodium-ion battery. *Chem. Commun.* **50**: 14029-14032.